

Experimental and density functional theory (DFT) studies on (*E*)-2-Acetyl-4-(4-nitrophenyldiazenyl) phenol

Serap Yazıcı^{a,*}, Çiğdem Albayrak^b, İsmail Gümrükçüoğlu^a, İsmet Şenel^a, Orhan Büyükgüngör^a

^a Department of Physics, Faculty of Arts and Sciences, Ondokuz Mayıs University, 55139 Kurupelit-Samsun, Turkey

^b Faculty of Education, Sinop University, 57000 Sinop, Turkey

ARTICLE INFO

Article history:

Received 5 October 2010

Received in revised form 3 November 2010

Accepted 3 November 2010

Available online 3 December 2010

Keywords:

Diazenyl

X-ray analysis

Nonlinear optical properties

Frontier molecular orbitals

Density functional theory (DFT)

Molecular Electrostatic potential (MEP)

ABSTRACT

A suitable single crystal of (*E*)-2-Acetyl-4-(4-nitrophenyldiazenyl) phenol, formulated as C₁₄H₁₁N₃O₄, (I), reveals that the structure is adopted to its *E* configuration and molecules are linked by C—H...O hydrogen bonds. The title compound which has been characterized by IR, UV and single crystal X-ray diffraction analysis at 150 K crystallizes in the monoclinic space group *C* 2/*c* with *a* = 12.8640(8) Å, *b* = 7.3264(3) Å, *c* = 26.9330(17) Å, $\alpha = 90^\circ$, $\beta = 93.052(5)^\circ$, $\gamma = 90^\circ$, *Z* = 7. The molecular structure and geometry have also been optimized using B3LYP density functional theory method employing the 6-31G (d, p) basis set. To acquire lowest- energy molecular conformation of the title molecule, the selected torsion angle is varied every 10° and molecular energy profile is calculated from −180° to +180°. Furthermore, the molecular electrostatic potential (MEP), frontier molecular orbitals (FMO) analysis, nonlinear optical properties (NLO) and thermodynamic properties for the title molecule are also described from the computational process.

© 2010 Elsevier B.V. All rights reserved.

1. Introduction

Azo compounds are the oldest and largest class of industrial synthesized organic dyes due to their versatile application in various fields, such as dyeing textile fiber, biomedical studies, advanced application in organic synthesis and high technology areas such as laser, liquid crystalline displays, electro-optical devices and ink-jet printers [1–3]. All of azo compounds contain at least one azo (—N=N—) group, which links two sp²-hybridized C atoms in the structures. Almost all colours have been obtained by increasing number of azo groups and attaching substitute groups to aromatic rings that linked to azo groups [4]. Furthermore, azo compounds are a model of the photochromic compounds that display *cis* and *trans* isomerism [5,6]. The *trans*-to-*cis* isomerization occurs by photoirradiation with UV light and *cis*-to-*trans* isomerization proceeds with blue light irradiation or by heating. It is generally accepted that their *trans* forms are thermodynamically more stable than their *cis* form [7,8].

In this paper, we report the molecular and crystal structure of (*E*)-2-Acetyl-4-(4-nitrophenyldiazenyl) phenol, together with the IR, UV and single crystal X-ray diffraction studies. The conformational analysis of the title molecule with respect to the selected torsion angle is achieved by DFT. Besides these, the molecular

structure and geometry, FMOs, MEP, total molecular energies, dipole moments, NLO and thermodynamic properties have also been studied using the DFT/ B3LYP employing the 6-31G (d, p) basis set. The results obtained from theoretical calculations and experiments are compared in this study.

2. Experimental

2.1. Synthesis

The compound was prepared by reflux a mixture of a solution containing 4-nitroaniline (1.08 g, 7.8 mmol), water (20 ml) and concentrated hydrochloric acid (1.97 ml, 23.4 mmol) was stirred until a clear solution was obtained. This solution was cooled down to 0–5 °C and a solution of sodium nitrite (0.75 g, 7.8 mmol) in water was added dropwise while the temperature was maintained below 5 °C. The resulting mixture was stirred for 30 min in an ice bath. 2-Hydroxyacetophenone (1.067 g, 7.8 mmol solution (pH 9) was gradually added to a cooled solution of 4-nitrobenzenediazonium chloride, prepared as described above, and the resulting mixture was stirred at 0–5 °C for 2 h in ice bath. The product was recrystallized from acetic acid to obtain solid (*E*)-2-Acetyl-4-(4-nitrophenyldiazenyl) phenol. Crystals of (*E*)-2-Acetyl-4-(4-nitrophenyldiazenyl) phenol (Fig. 1) were obtained after one day by slow evaporation from DMSO (yield 88%, m.p. = 452–454 K).

* Corresponding author. Fax: +90 0362 4576092.

E-mail address: yserap@omu.edu.tr (S. Yazıcı).

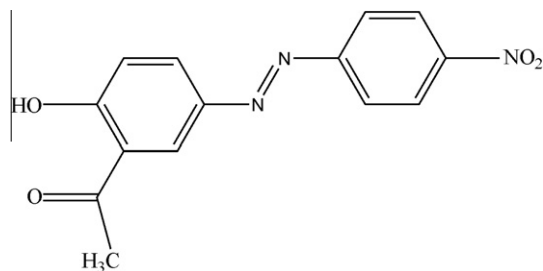


Fig. 1. Chemical diagram of (*E*)-2-Acetyl-4-(4-nitrophenyl)diazenyl phenol.

2.2. Instrumentation

The FT-IR spectrum of the title compound was recorded in the 4000–400 cm^{-1} region with a Bruker Vertex 80 V FT-IR spectrometer using KBr pellets. Absorption spectra were determined on Unicam UV-Vis spectrometer.

2.3. X-ray crystallography

A brown crystal of size $0.420 \times 0.317 \times 0.130 \text{ mm}^3$ was picked for the crystallographic study. All diffraction measurements were performed at low temperature (150 K) using graphite monochromated Mo $K\alpha$ radiation ($\lambda = 0.71073 \text{ \AA}$) with a STOE IPDS II diffractometer. The systematic absences and intensity symmetries indicated the monoclinic $C2/c$ space group. Correction for absorption $\mu = 0.11$, by comparison of the intensities of equivalent reflections, was applied using X-RED software [9] and cell parameters were determined by using X-AREA software [9]. The structure was solved by direct methods using SHELXS 97 [10] and refined by a full-matrix least-squares method using the program SHELXL 97 [10]. All non-hydrogen atoms were refined anisotropically and the positions of H atoms, except for O-bound H atom, were obtained from difference Fourier map of electron density in the unit cell (C–H distance of 0.96 \AA for methyl and hydroxyl groups, 0.93 \AA for aromatic groups). The $U_{\text{iso}}(\text{H})$ values were fixed to $1.2U_{\text{eq}}(\text{C})$ (for aromatic CH) and $1.5U_{\text{eq}}(\text{C})$ (for CH_3 and OH). Details of crystal data, data collection, structure solution, and refinement are listed in Table 1.

Table 1
Crystal data and structure refinement parameters for the title compound.

Chemical formula	$\text{C}_{14}\text{H}_{11}\text{N}_3\text{O}_4$
Colour/shape	Brown/plate
Formula weight	285.25
Temperature	150 K
Crystal system	Monoclinic
Space group	$C2/c$
Unit cell parameters	$a = 12.8640(8) \text{ \AA}$ $b = 7.3264(3) \text{ \AA}$ $c = 26.9330(17) \text{ \AA}$ $\alpha = 90^\circ$ $\beta = 93.052(5)^\circ$ $\gamma = 90^\circ$
Volume	$2534.8(3) \text{ \AA}^3$
Z	7
Density	1.495 g/cm^3
Absorption coefficient	0.11 mm^{-1}
$T_{\text{min}}, T_{\text{max}}$	0.930, 0.993
Diffractometer/meas. meth.	STOE IPDS 2 / ω -scan
θ range for data collection	$1.51\text{--}26.76^\circ$
Unique reflections measured	6261
Independent/observed reflections	2456/1919
Data/restraints/parameters	1919/0/194
Goodness of fit on F^2	1.024
Final R indices [$I > 2\sigma(I)$]	$R_1 = 0.0364$, $wR_1 = 0.0970$
R indices (all data)	$R_2 = 0.0477$, $wR_2 = 0.1013$

2.4. Computational procedures

The molecular structure of the title molecule is optimized by the DFT calculations with a hybrid functional B3LYP (Becke's Three parameter Hybrid Functional using the LYP Correlation Functional) at 6-31G (d, p) basis set [11,12] and all of the calculations were carried out using Gaussian 03 program package [13]. The vibrational frequencies for optimized molecule have also been calculated at the same level of the theory and achieved frequencies were scaled by 0.9627 [14]. The electronic absorption spectra for optimized molecule calculated with the time dependent density functional theory (TD-DFT) at B3LYP/6-31G (d, p) level. To elucidate conformational features of the molecule, the selected degree of torsional freedom, T (C2-C1-N1-N2), was varied from -180° to $+180^\circ$ in every 10° and the molecular energy profile was obtained with the B3LYP/6-31G (d, p) method. In addition, FMO, MEP, NLO and thermodynamic properties were performed with the same level of theory.

3. Results and discussion

3.1. Description of the crystal structure

The molecular structure, an ORTEP 3 [15] view of which is shown Fig. 2, crystallizes in the monoclinic space group $C2/c$ with seven molecules in the unit cell. The compound has two aromatic rings and an azo moiety. In the molecule, the aromatic rings which adopt (*E*) configuration with respect to the $\text{N}=\text{N}$ double bond, are almost coplanar with a dihedral angle of $2.62(2)^\circ$. In the azo group, while the N1-C1 and N2-C7 bond distances are $1.419(1) \text{ \AA}$ and $1.421(1) \text{ \AA}$, respectively, the $\text{N1}=\text{N2}$ bond length is $1.262(1) \text{ \AA}$ and these values are satisfactory agreement with found of those in the literature [16–18]. N3-C10 , N3-O1 and N3-O2 bond distances in the molecule are compared well with the values reported previously [19]. The C13-O4 bond which has distance of $1.234(1) \text{ \AA}$ is also consistent with the value of the $\text{C}=\text{O}$ double bond in carbonyl compounds [20]. As a result of the delocalization of the electron density in the azo bridge, C1-N1-N2-N7 , C2-C1-N1-N2 and N1-N2-C7-C8 torsion angles are $-179.4(1)^\circ$, $178.8(1)^\circ$ and $-179.1(1)^\circ$, respectively.

As can be seen in Fig. 2, atom H3 bonded to O3 forms a strong intramolecular hydrogen bond with atom O4 [$\text{D}\cdots\text{A} = 2.551(1) \text{ \AA}$] and this hydrogen bond generates an $\text{S}(6)$ ring motif. The sum of the van der Waals radii of two O atoms (3.04 \AA) is significantly longer than the intramolecular $\text{O}\cdots\text{O}$ hydrogen bond length [21]. The crystal packing of the title molecule is stabilized by two intermolecular $\text{C-H}\cdots\text{O}$ hydrogen bonds, one of them is between the atom C9 and oxygen of the carbonyl group (O4) and the other is between the atom C8 and oxygen of the nitro group (O2). These intermolecular interactions link neighbouring molecules in three dimensions (Fig. 3) (Table 2). In addition to these interactions, van der Waals forces should be effective on the crystal packing of the title azo dye.

3.2. Theoretical structure and conformation analysis

Some structural parameters obtained experimentally and calculated theoretically by B3LYP/6-31G (d, p) are given in Table 3 for comparison. The differences observed between the experimental and calculated parameters are due to the ignored effects. These effects are the intermolecular interactions which the theoretical methods cannot take into account. While the experimental results belong to the solid state, the calculated results belong to the isolated gaseous phase. The maximum difference between the experimental observation and those obtained from the theoretical

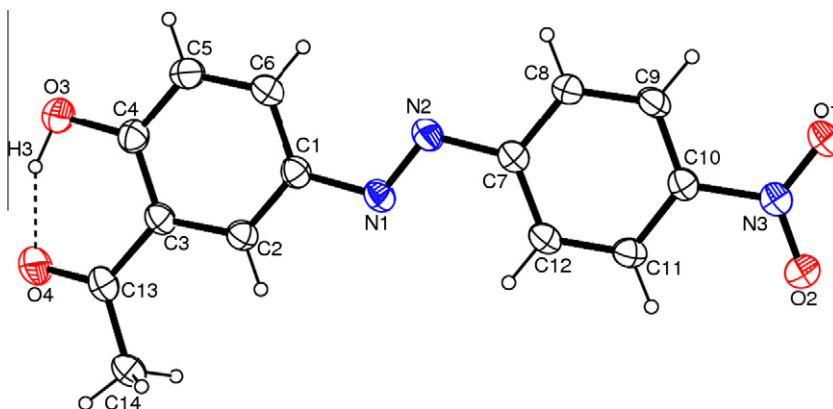


Fig. 2. Ortep three diagram for (*E*)-2-Acetyl-4-(4-nitrophenyldiazenyl) phenol, with the atom numbering scheme.

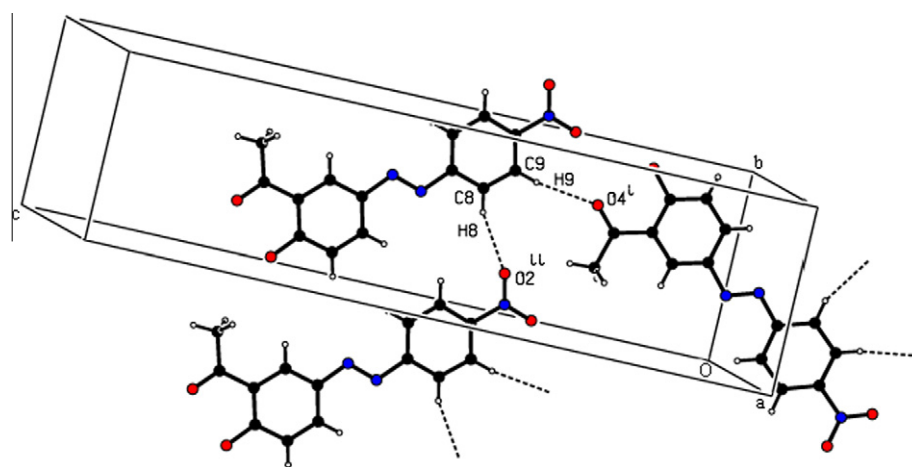


Fig. 3. A partial packing diagram of (*E*)-2-Acetyl-4-(4-nitrophenyldiazenyl) phenol.

Table 2
Hydrogen-bond geometry (Å, °).

D—H...A	D—H	H...A	D...A	D—H...A
O3—H3...O4	0.96(3)	1.65(2)	2.5509(15)	154(2)
C9—H9...O4 ^a	0.93	2.57	3.4856(17)	170
C8—H8...O2 ^b	0.93	2.49	3.3199(16)	149

^a Symmetry code: $x, 1 - y, -1/2 + z$.

^b Symmetry code: $x, 1 + y, z$.

Table 3
Selected molecular structure parameter for the title compound.

	X-ray	DFT		X-ray	DFT
<i>Bond lengths</i> (Å)		<i>Bond angles</i> (°)			
C1—N1	1.419(1)	1.405	C1—N1—N2	113.4(1)	115.2
N1—N2	1.262(1)	1.264	N1—N2—C7	114.4(1)	114.3
N2—C7	1.421(1)	1.417	N2—C7—C8	114.9(1)	115.3
O3—C4	1.341(1)	1.330	O3—C4—C5	117.4(1)	118.1
O4—C13	1.234(1)	1.241	O3—C4—C3	122.6(1)	122.2
C3—C13	1.477(1)	1.473	O4—C13—C3	119.4(1)	120.6
C13—C14	1.486(2)	1.512	C3—C13—C14	120.1(1)	120.3
C10—N3	1.463(1)	1.470	C10—N3—O1	118.2(1)	117.7
N3—O1	1.220(1)	1.231	C10—N3—O2	118.6(1)	117.7
N3—O2	1.224(1)	1.231	O1—N3—O2	123.1(1)	124.6
<i>Torsion angles</i> (°)					
C2—C1—N1—N2	178.8(1)	180.0	O3—C4—C3—C13	−1.7(1)	0.0
C7—N2—N1—C1	−179.4(1)	180.0	O1—N3—C10—C9	4.4(2)	0.0
N1—N2—C7—C8	−179.1(1)	180.0	O2—N3—C10—C11	4.3(1)	0.0

calculations is 0.0264 Å for bond distances and 1.7497° for bond angles. Besides these, in the optimized molecule, dihedral angle between the hydroxyl attached ring and NO₂ attached ring is 0.018°. Namely, the optimized geometry with B3LYP is preferred more planar conformation than X-ray geometry.

In order to define conformational flexibility of the title molecule, the energy profile as a function of C2—C1—N1—N2 torsion angle was achieved with B3LYP/6-31G (d,p) method (Fig. 4). According to X-ray crystallographic study *T* (C2—C1—N1—N2) is 178.8(1)° and 180.0° for DFT. The conformational energy profile shows two maxima near 90° and −90°. The aromatic rings are nearly perpendicular at these values of selected torsion angle. The energy barriers may be due to the steric interactions between the π electrons of the two aromatic rings. It is clear from Fig. 5, there are three local minima observed at 180°, 0° and −180° for *T* (C2—C1—N1—N2) and these are most stable conformers for this torsion angle. The DFT optimized geometry of the crystal structure is coplanar at these values of selected torsion angle.

3.3. Vibrational spectra

The harmonic vibrational frequencies for (*E*)-2-Acetyl-4-(4-nitrophenyldiazenyl) phenol have been calculated by using DFT method at 6-31G (d,p) level. There are no imaginary values for any frequencies, indicating that is the minimum energy structure at this level of theory. In order to compare the theoretical results with experimental values of those, all of the calculated frequencies are scaled by 0.9627 for B3LYP/6-31G (d,p). Some characteristic IR

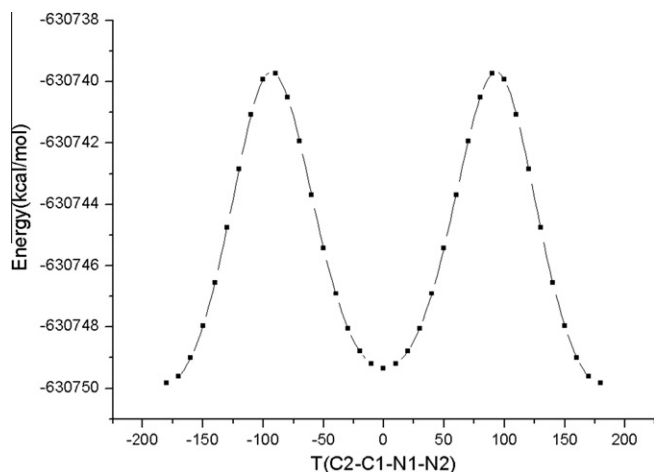


Fig. 4. Molecular energy profile using DFT against the selected torsional degree of freedom.

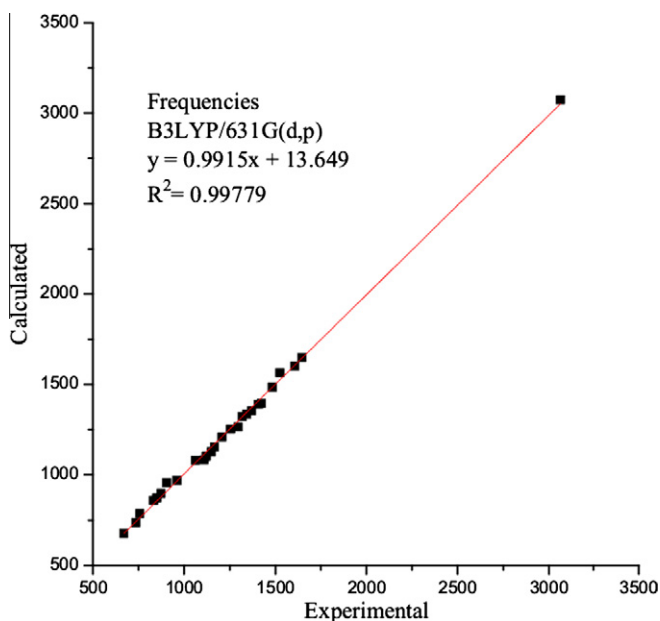


Fig. 5. Correlation graphic of calculated and experimental frequencies of the title compound.

bands for the title azo dye has given in Table 4 and the correlation graphic which described harmony between the calculated and experimental frequencies is plotted (Fig. 5). As can be seen from Fig. 5, experimental fundamentals have a better correlation with B3LYP.

Table 4
Characteristic IR absorption bands of the title molecule.

Assignments	Experimental (cm ⁻¹)	Calculated (cm ⁻¹)
O–H str.	2000–3000	3078
C=O str.	1647	1651
N=N str.	1424	1451
C–O str.	1206	1301
O–H bend.	1318	1567
C–N (nitro) str.	1370	1340
N–O (Symm) str.	1342	1553
N–O (asymm) str.	1524	1603

str.: stretching, bend.: bending.

In the IR spectral data of the molecule which obtained from 2-hydroxy acetophenone two bands are extremely characteristic. These are $\nu(\text{C}=\text{O})$ and $\nu(\text{N}=\text{N})$ stretching bands. While the experimental N=N and C=O stretching modes were observed at 1424 and 1647 cm⁻¹ [22], respectively. The same bands were calculated as 1451 and 1651 cm⁻¹, respectively. The nitro group in the studied molecule was denoted two very strong absorption bands in the experimental and theoretical IR spectral analysis. These bands that attributed to antisymmetric and symmetric NO₂ stretching vibrations were observed at 1524, 1342 cm⁻¹ for experimental that have been calculated with B3LYP at 1603, 1553 cm⁻¹, respectively. Because of the participation of the carbonyl group in hydrogen bonding, the experimental frequencies were shifted towards lower frequencies than the theoretical values of those. Due to the same reason, while O–H stretching band experimentally located at the region 2000–3000 cm⁻¹, its theoretical value calculated as 3078 cm⁻¹. The above conclusions are in good agreement with the literature values [23,24].

3.4. Electronic absorption spectra

The electronic absorption bands which have azo groups obtained from UV–Vis spectroscopy. The UV–Vis electronic absorption spectra of the title compound in different solvents had been recorded in the previous study [22]. We have also calculated electronic absorption spectra of (*E*)-2-Acetyl-4-(4-nitrophenyldiazenyl) phenol in three different solvents (DMSO, EtOH and CHCl₃) using TD-DFT at B3LYP/6-31G (d, p) level by adding the polarizable continuum model (PCM). The theoretical and experimental absorption wavelengths are compared in Table 5. In the evaluation of the results was based on the oscillator strengths (*f*-value) which greater than 0.1. It is well known that $\pi \rightarrow \pi^*$ transition is shifted to long wavelength with increasing the solvent polarity. The reason of this shifting, the dipole moment of solvent is produced dipole moment over the solute matter. Consequently, the energy of the π^* orbital is decreased. As can be seen from Table 5, while excitation energies decrease absorption wavelengths increase with increasing polarity of the solvents in the title molecule too. In the calculated UV–Vis spectrum of the title molecule absorption bands occur at 421.13 nm for DMSO, 417.59 nm for EtOH and 415.64 nm for CHCl₃, arising from HOMO \rightarrow LUMO transition.

3.5. Frontier molecular orbitals (FMOs)

The highest occupied molecular orbitals (HOMOs) and the lowest-lying unoccupied molecular orbitals (LUMOs) are named as frontier molecular orbitals (FMOs). The FMOs play an important role in the electric and optical properties, as well as in UV–Vis spectra and chemical reactions [25]. The distributions of the HOMO-1, HOMO, LUMO and LUMO+1 orbitals computed at the B3LYP/6-31G (d, p) level for the title molecule are illustrated in Fig. 6. The calculations indicate that the title compound have 74 occupied MOs. While the HOMO and LUMO are localized on almost the whole molecule, HOMO-1 and LUMO+1 are localized on the azo bridge and the carbonyl attached ring, respectively. Both the HOMOs and the LUMOs are mostly π -antibonding type orbitals. Since the HOMO–LUMO energy separation has been used as a simple indicator of kinetic stability it can be said that the title molecule which has a large HOMO–LUMO gap, 3.399 eV, implies high kinetic stability and low chemical reactivity [26,27].

3.6. Molecular electrostatic potential

The molecular electrostatic potential isosurface superimposed onto the total electronic density. The value of the molecular electrostatic potential, $V(r)$, created by a molecular system at a point

Table 5
Theoretic and experimental absorption wavelengths for the title compound.

	Oscillator strengths (<i>f</i>)	Theoretical wavelengths (λ), nm	Experimental wavelengths (λ), nm	Excitation energies, eV
Chloroform ($\epsilon = 4.9$)	1.0334	415.64	366	2.9830
Ethanol ($\epsilon = 24.55$)	0.9920	417.59	365	2.9690
DMSO ($\epsilon = 46.7$)	1.0221	421.13	373	2.9441

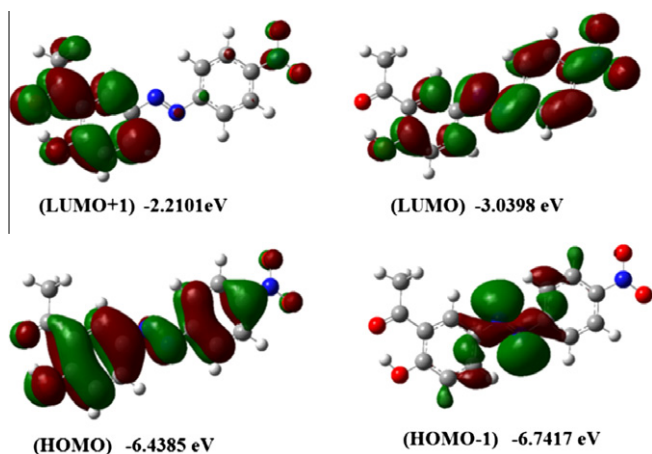


Fig. 6. Molecular orbital surfaces and energies for the HOMO-1, HOMO, LUMO and LUMO+1 of the title compound.

r gives the electrostatic energy on a unit positive charge located at r . The molecular electrostatic potential (MEP) is a useful property to study reactivity given that an approaching electrophile will be attracted to negative regions (particularly to points with most negative values), where the electron distribution effect is dominant. Experimental $V(r)$ computed with electron densities obtained from X-ray diffraction data has been used to explore the electrophilicity of hydrogen bonding functional groups [28]. In the majority of the MEPs, while the maximum positive region which preferred site for nucleophilic attack indications as blue colour, the maximum negative region which preferred site for electrophilic attack indications as red colour. The study of experimental and theoretical $V(r)$ shows that H-donor and H-acceptor properties of molecules are revealed by positive and negative regions, respectively, so that the formation of a H-bond can be regarded as the consequence of a complementarity between the electrostatic potentials [28].

In the present study, the molecular electrostatic potential of (*E*)-2-Acetyl-4-(4-nitrophenyldiazenyl) phenol depicted in Fig. 7. Negative regions are associated with O1, O2, O3 and O4 with values around -0.047 , -0.047 , -0.026 and -0.029 a.u., respectively. So, it is expected that the most preferred region for electrophilic attack is that around O1 and O2. However, the most maximum positive region is localized on atom C14 which a member of methyl group with a value of 0.035 a.u. Therefore, it would be predicted that the preferred site for nucleophilic attack will be C14.

3.7. Energies and dipole moments

In order to evaluate the energetic behavior of the title compound in solvent media, we carried out calculations in vacuo and in various organic solvents (chloroform, ethanol and dimethylsulfoxide, DMSO). The calculated total molecular energies, frontier orbital energies and dipole moments using the PCM (polarizable continuum model) [29] by B3LYP/6-31G (d,p) are listed in Table 6. As seen in table, with the rising polarity of the solvent total molecular energy of the title molecule diminishes and so the stability of the structure increases. Due to the inductive solvent

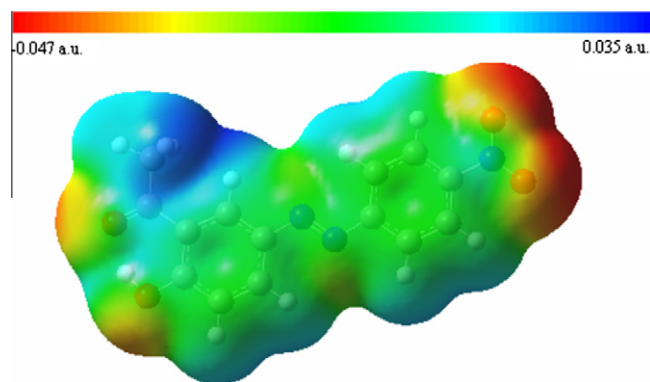


Fig. 7. Molecular electrostatic potential map calculated at B3LYP/6-31G (d,p).

polarization effects in the polar solvents the dipole moment increases with the polarity of the solvent. Furthermore, the energy gap (ΔE) between the HOMO and LUMO of the title compound decreases with increasing polarity of the solvent.

3.8. Nonlinear optical effects

Nonlinear optical (NLO) effects arise from the interactions of electromagnetic fields in various media to produce new fields altered in phase, frequency, amplitude or other propagation characteristics from the incident fields. The search of new materials exhibiting efficient nonlinear optical (NLO) properties has been of great interest in the recent years because of their potential applications in telecommunication, data storage and optical signal processing [30–36]. It is known that the magnitude of the polarizability and the first static hyperpolarizability of push–pull molecular systems is dependent on the efficiency of electronic communication between donor and the acceptor groups as that will be the key to intra molecular charge transfer [37].

The polar properties of the title molecule were calculated at the B3LYP/6-31G (d,p) level using the Gaussian 03 W program package. The calculated values of electronic dipole moment, μ , polarizability, α , and the first hyperpolarizability, β for the title compound which including NO_2 as the donor group are, 3.9493 Debye, 34.7592 \AA^3 and $70.9379 \times 10^{-30} \text{ cm}^5/\text{esu}$, respectively. It is well known that the substituents influence the polarity of the molecules. The high value of the first hyperpolarizability of the title compound can be seen a result of the resonance effect of nitro group.

3.9. Thermodynamic properties

In order to determinate the thermodynamic behavior of the title compound, in the light of vibrational analysis and statistical thermodynamics, the standard thermodynamic functions: molar heat capacities ($C_{p,m}^0$), entropies (S_m^0) and enthalpies (H_m^0), were reached at the same level of theory and listed in Table 7. As seen from Table 7, the standard thermodynamic functions increase at any temperature from 100.00 to 500.00 K, due to the intensities of molecular vibration increase as temperature increases. The

Table 6

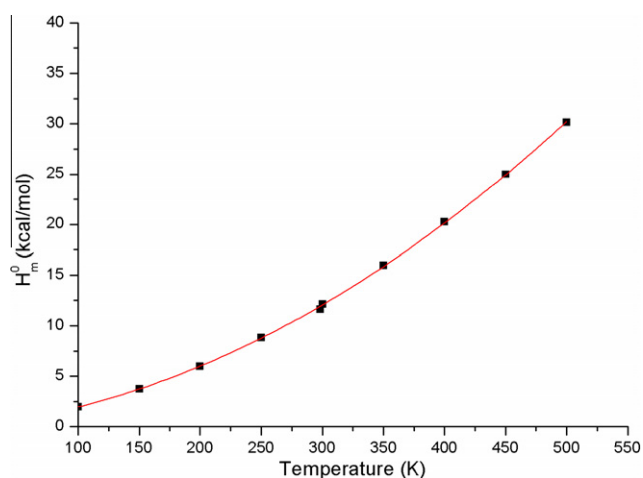
Calculated energies, dipole moments and frontier orbital energies for the title compound.

	Gas phase ($\epsilon = 1$)	Chloroform ($\epsilon = 4.9$)	Ethanol ($\epsilon = 24.55$)	DMSO ($\epsilon = 46.7$)
E_{TOTAL} (eV)	-27352.11496402	-27352.47387169	-27352.56739034	-27352.56753293
E_{HOMO} (eV)	-6.4383	-6.3062	-6.2701	-6.2693
E_{LUMO} (eV)	-3.0397	-3.0156	-3.0137	-3.0156
ΔE (eV)	3.399	3.291	3.256	3.254
μ (D)	3.9521	4.5126	4.6659	4.6853

Table 7

Thermodynamic properties at different temperatures at the B3LYP/6-31G (d, p) level for the title compound.

T (K)	H_m^0 (kcal/mol)	$C_{p,m}^0$ (cal/mol K)	S_m^0 (cal/mol K)
100	1.989	28.459	90.987
150	3.738	38.356	105.189
200	6.012	48.670	118.199
250	8.808	59.187	130.632
298.150	11.650	66.900	139.906
300	12.127	69.556	142.707
350	15.954	79.434	154.485
400	20.257	88.579	165.964
450	24.996	96.876	177.118
500	30.129	104.314	187.927

**Fig. 8.** Correlation graphic of enthalpy and temperature for the title molecule.

correlation equations between these thermodynamic properties as a function of the temperature T are as follows and the correlation graphics of those show in Figs. 8–10.

$$C_{p,m}^0 = 4.66575 + 0.23844T - 7.56983 \times 10^{-5}T^2$$

$$(R^2 = 0.99941)$$

$$S_m^0 = 63.38186 + 0.28802T - 7.83966 \times 10^{-5}T^2$$

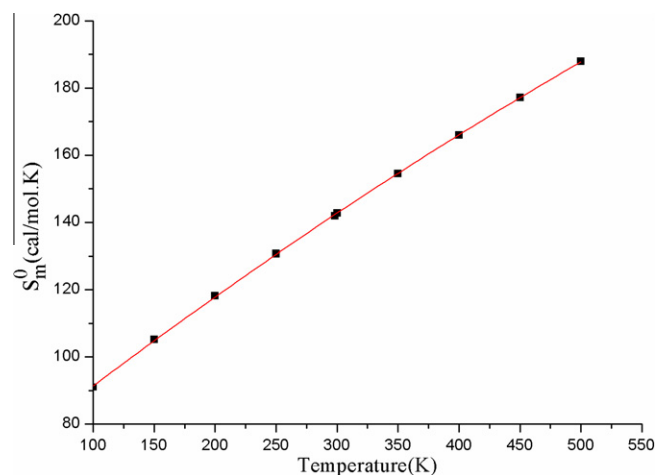
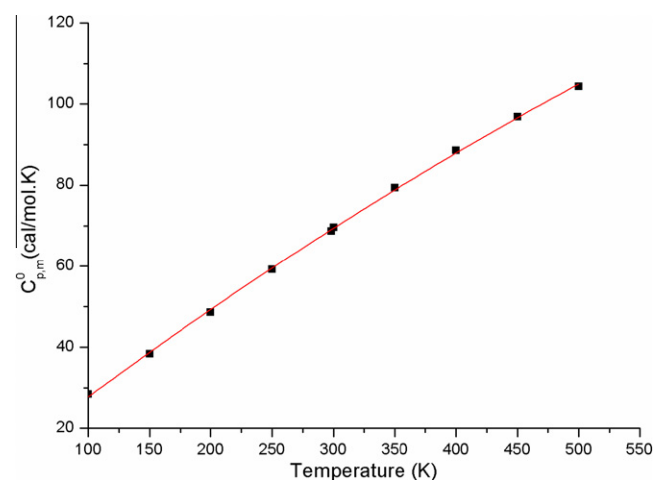
$$(R^2 = 0.99991)$$

$$H_m^0 = -0.06797 + 0.01025T + 1.00681 \times 10^{-4}T^2$$

$$(R^2 = 0.99979)$$

4. Conclusion

In the present work, the synthesis, FT-IR and UV-Vis, crystal and molecular structure determined by single crystal X-ray diffraction as well as DFT calculations, of (*E*)-2-Acetyl-4-(4-nitrophenyldiazenyl) phenol are reported. The comparisons between the calculated results and the X-ray experimental data indicate that B3LYP/6-31G (d, p) method shows a good agreement with

**Fig. 9.** Correlation graphic of entropy and temperature for the title molecule.**Fig. 10.** Correlation graphic of heat capacity and temperature for the title molecule.

the experimental results. Although there are some differences between the theoretical and experimental frequencies, due to the participation of the carbonyl group in hydrogen bonding we can generally say that there is a good linear correlation between them. Molecular electrostatic potential map shows several possible sites for electrophilic attack and shows a possible site for nucleophilic attack. These sites may provide information about the possible reaction regions for the title structure. The total molecular energy of the title compound decreases with increasing polarity of the solvent and the stability of the molecule increases. The correlations between the statistical thermodynamics and temperature are also obtained. It was seen that the heat capacities, entropies and enthalpies increase with the increasing temperature owing to the intensities of the molecular vibrations increase with increasing temperature. This study also demonstrates that the effect of the

presence of a nitro group in the material enhances the nonlinear optical property.

Supplementary data

CCDC 751379 contains the supplementary crystallographic data for this paper. These data can be obtained free of charge via www.ccdc.cam.ac.uk/data_request/cif, by emailing data_request@ccdc.cam.ac.uk, or by contacting The Cambridge Crystallographic Data Centre, 12, Union Road, Cambridge CB2 1EZ, UK; fax: +44 1223 336033.

Acknowledgements

The authors wish to acknowledge the Faculty of Arts and Sciences, Ondokuz Mayıs University, Turkey, for the use of the STOE IPDS 2 diffractometer (purchased under grant F.279 of the University Research Fund).

References

- [1] S.C. Catino, R.E. Farris (Eds.), *Concise Encyclopedia of Chemical Technology*, John Wiley & Sons, New York, 1985.
- [2] K. Venkataraman, *The Chemistry of Synthetic Dyes*, Academic Press, New York and London, 1970 (Chapter 6).
- [3] R. Egli, A.P. Peter, H.S. Freeman, *Colour Chemistry the Design and Synthesis of Organic Dyes and Pigments*, Elsevier, London, 1991 (Chapter 7).
- [4] K.H. Saunders, R.L.M. Allen (Eds.), *Aromatic Diazo Compounds*, third ed., Edward Arnold, London, 1985.
- [5] M.J. Lee, B.W. Yoo, S.T. Shin, S.R. Keum, *Dyes Pigm.* 51 (2001) 15.
- [6] N. Tamai, H. Miasaka, *Chem. Rev.* 100 (2000) 1875.
- [7] M. Azuki, K. Morihashi, T. Watanabe, O. Taskahashi, *J. Mol. Struct. Theochem.* 542 (2001) 255.
- [8] S.Y. Grebenkin, B.V. Bolshakov, *J. Photochem. Photobiol. A: Chem.* 122 (1999) 205.
- [9] Stoe & Cie, X-AREA (Version 1.18) and X-RED32 (Version 1.04), Darmstadt, Germany, 2002.
- [10] G.M. Sheldrick, SHELXS 97 and SHELXL 97, University of Göttingen, Germany, 1997.
- [11] A.D. Becke, *J. Chem. Phys.* 98 (1993) 5648.
- [12] C. Lee, W.T. Yang, R.G. Parr, *Phys. Rev. B* 37 (1988) 785.
- [13] M.J. Frisch, G.W. Trucks, H.B. Schlegel, G.E. Scuseria, M.A. Robb, J.R. Cheeseman, J.A. Montgomery, T.J. Vreven, K.N. Kudin, J.C. Burant, J.M. Millam, S.S. Iyengar, J. Tomasi, V. Barone, B. Mennucci, M. Cossi, G. Scalmani, N. Rega, G.A. Peterson, H. Nakatsuji, M. Hada, M. Ehara, K. Toyota, R. Fukuda, J. Hasegawa, M. Ishida, T. Nakajima, Y. Honda, O. Kitao, H. Nakai, M. Klene, X. Li, J.E. Knox, H.P. Hratchian, J.B. Cross, C. Adamo, J. Jaramillo, R. Gomperts, R.E. Stratmann, O. Yazyev, A.J. Austin, R. Cammi, C. Pomelli, J.W. Ochterski, P.Y. Ayala, K. Morokuma, G.A. Voth, P. Salvador, J.J. Dannenberg, V.G. Zakrzewski, A. Dapprich, A.D. Daniels, M.C. Strain, O. Farkas, D.K. Malick, A.D. Rabuck, K. Raghavachari, J.B. Foresman, J.V. Ortiz, Q. Cui, A.G. Baboul, S. Clifford, J. Cioslowski, B.B. Stefanov, G. Liu, A. Liashenko, P. Piskorz, I. Komaromi, R.L. Martin, D.J. Fox, T. Keith, M.A. Al-Laham, C.Y. Peng, A. Nanayakkara, M. Challacombe, P.M.W. Gill, B. Johnson, W. Chen, M.W. Wong, C. Gonzalez, J.A. Pople, Gaussian 03, Revision E.01, Gaussian, Inc., Pittsburgh, PA, 2003.
- [14] J.P. Merrick, D. Moran, L. Radom, *J. Phys. Chem. A* 111 (2007) 11683.
- [15] L.J. Farrugia, *J. Appl. Cryst.* 30 (1997) 565.
- [16] S. Yazıcı, Ç. Albayrak, I.E. Gümrükçüoğlu, İ. Şenel, O. Büyükgüngör, *Acta Crystallogr. E* 66 (2010) o559.
- [17] Ç. Albayrak, M. Odabaşoğlu, O. Büyükgüngör, H. Goesmann, *Acta Crystallogr. C* 59 (2003) o234.
- [18] F.H. Allen, O. Kennard, D.G. Watson, L. Brammer, A.G. Orpen, J. Chem. Soc. Perkin Trans. 2 (1987) 1.
- [19] B. Koşar, Ç. Albayrak, I. Gümrükçüoğlu, O. Büyükgüngör, *Acta Crystallogr. E* 63 (2007) o4772.
- [20] M.G. Loudon, *Study Guide and Solutions Manual to Accompany Organic Chemistry*, fourth ed., Oxford, 2002.
- [21] A. Bondi, *J. Phys. Chem.* 68 (1964) 441.
- [22] Ç. Albayrak, I.E. Gümrükçüoğlu, M. Odabaşoğlu, N.O. Iskeleli, E. Ağar, *J. Mol. Struct.* 932 (2009) 43.
- [23] H. Karaer, I.E. Gümrükçüoğlu, *Turk. J. Chem. Cryst.* 23 (1999) 61.
- [24] F. Karci, A. Demirçali, İ. Şener, T. Tilki, *Dyes Pigm.* 71 (2006) 90.
- [25] I. Fleming, *Frontier Orbitals and Organic Chemical Reactions*, Wiley, London, 1976.
- [26] K.H. Kim, Y.K. Han, J. Jung, *Theor. Chem. Accounts* 113 (2005) 233.
- [27] J. Aihara, *Theor. Chem. Accounts* 102 (1999) 134.
- [28] S.J. Grabowski, J. Leszczynski, Unrevealing the nature of hydrogen bonds: π -electron delocalization shapes H-bond features, in: J. Slawomir (Ed.), *Hydrogen Bonding – New Insights*, Grabowski Kluwer, Academic Publishers, 2006.
- [29] J. Tomasi, B. Mennucci, R. Cammi, *Chem. Rev.* 105 (2005) 2999.
- [30] D.S. Chemia, J. Zyss, *Non linear Optical Properties of Organic Molecules and Crystal*, Academic Press, New York, 1987.
- [31] M.D. Aggarwal, J. Stephens, A.K. Batra, R.B. Lal, *J. Optoelectron. Adv. Mater.* 5 (2003) 555.
- [32] R. Ittyachan, P. Sagayaraj, *J. Cryst. Growth* 249 (2003) 557.
- [33] M.K. Marchewka, S. Debrus, A. Pietraszko, A.J. Barnes, H.J. Ratajczak, *J. Mol. Struct.* 656 (2003) 265.
- [34] J. Zyss, *Molecular Non linear Optics*, Academic Press, Boston, 1994.
- [35] K. Clays, B.J. Coe, *Chem. Mater.* 15 (2003) 642.
- [36] A. Ben Ahmed, H. Feki, Y. Abid, C. Minnot, *Spectrochim. Acta Part A: Mol. Biomol. Spectrosc.* 75 (2010) 1315.
- [37] K. Amila, K.M. Jeewandara, de S. Nalin, *J. Mol. Struct. Theochem.* 686 (2004) 131.